Glass Transition Temperature and Density Scaling in Cumene at Very High Pressure

T. C. Ransom and W. F. Oliver

Phys. Rev. Lett. **119**, 025702 — Published 14 July 2017

DOI: 10.1103/PhysRevLett.119.025702

Glass Transition Temperature and Density Scaling at Very High Pressure

T. C. Ransom and W. F. Oliver
Physics Department, University of Arkansas, Fayetteville, Arkansas 72701, USA

We present a new method that allows direct measurements of the glass transition temperature T_g at pressures up to 4.55 GPa in the glass-forming liquid cumene (isopropylbenzene). This new method uses a diamond anvil cell and can measure T_g at pressures of 10 GPa or greater. Measuring T_g at the glass→liquid transition involves monitoring the disappearance of pressure gradients initially present in the glass, but also takes advantage of the large increase in the volume expansion coefficient α_p at T_g as the supercooled or superpressed liquid is entered. Accurate $T_g(P)$ values in cumene allow us to show that density scaling holds along this isochronous line up to pressures much higher than any previous study, corresponding to a density increase of 29%. Our results for cumene over this huge compression range yield $\rho^\gamma/T = C$, where C is a constant and where $\gamma = 4.77 \pm 0.02$ for this non-associated glass-forming system. Finally, high-pressure cumene viscosity data from the literature taken at much lower pressures and at several different temperatures, corresponding to a large dynamic range of nearly 13 orders of magnitude, are shown to superimpose on a plot of η vs. ρ^γ/T for the same value of γ.

PACS numbers: 64.70.pm, 07.35.+k, 65.20.Jk, 66.20.Ej

Many liquids and polymers are readily cooled well below their freezing temperature T_m, exhibiting a dramatic increase of viscosity η and slowing down of structural relaxation time τ_α by many orders of magnitude upon approach to the glass transition temperature T_g, marked by $\eta = 10^{13}$ poise and $\tau_\alpha = 100$ s [1]. Though several theoretical approaches exist [2–8], a consensus for a microscopic description for this behavior remains elusive, and hence Philip Anderson's comment in 1995 that understanding the nature of glass and the glass transition is probably "the deepest and most interesting unsolved problem in solid state theory" [9] remains valid today. In addition to the traditional approach of glass formation by supercooling, it is also possible to achieve vitrification through superpressing, where densification drives the transition [10]. Any ultimate fundamental solution of the glass transition problem must describe phenomena associated with both pathways. Variable temperature and pressure depolarized light scattering showed over 20 years ago that τ_α is not driven by density alone; instead, it is controlled by the same combination of T and P (or T and ρ) as is viscosity [11]. Soon afterward, variable pressure quasielastic neutron scattering results gave intriguing hints of a scaling relation valid near the crossover line $P_c(T)$ in which glass-transition dynamics are governed by a constant parameter proportional to ρ^4/T for the van der Waals fragile glass-forming liquid *o*-terphenyl (oTP) [12]. Subsequent studies discovered that many glass-forming systems obey the more general scaling relation

$$x(\rho, T) = F(\rho^\gamma/T), \tag{1}$$

where x is τ_α or η, F is an unknown function, and γ is a material-dependent scaling exponent [10, 13–18]. This scaling, known as density scaling, allows dynamic measurements taken over a broad range of T and ρ to collapse onto a single master curve when plotted vs. ρ^γ/T.

Density scaling also allows researchers to construct isochoric plots or calculate isochoric derivatives and thus compare the relative importance of ρ and T independently [19–21], whereas isobaric cooling experiments always entangle both quantities via thermal contraction. It has helped lead to the classification of certain liquids as "strongly correlating" and the development of isomorph theory in which many properties of correlating liquids are invariant under conditions of constant ρ^γ/T [22–24]. Furthermore, the exponent γ is theorized to provide a critical quantitative connection between cooperative dynamics and the intermolecular potential [20, 25, 26]. Though this scaling behavior has been found to hold over broad dynamic ranges, most tests of Eq. (1) in glass-forming systems to date have been limited to pressures up to about 1 GPa, and hence relatively small compression ranges. This limitation has led to debate about whether the scaling variable truly requires a power law in density or if an alternative function such as one linear in density $(\rho - \rho^*)/T$, where ρ^* is a material constant, might equally suffice [10]; small density ranges have made it difficult to answer this question [19]. There is also recent computational evidence that power-law scaling breaks down in the high density limit [27], a result that can only be tested experimentally at very high pressures. A powerful approach to test Eq. (1) over broad density ranges is by measuring the P-dependence of T_g.

The $T_g(P)$ boundary represents an isochronous line at $\tau_\alpha(\rho_g, T_g) \approx 100$ s. For constant τ_α, Eq. (1) requires the constraint

$$C = \rho_g^\gamma/T_g, \tag{2}$$

where C is a constant along the $T_g(P)$ line. In this letter, we present the first direct measurements of $T_g(P)$ using a new technique in a high pressure diamond anvil

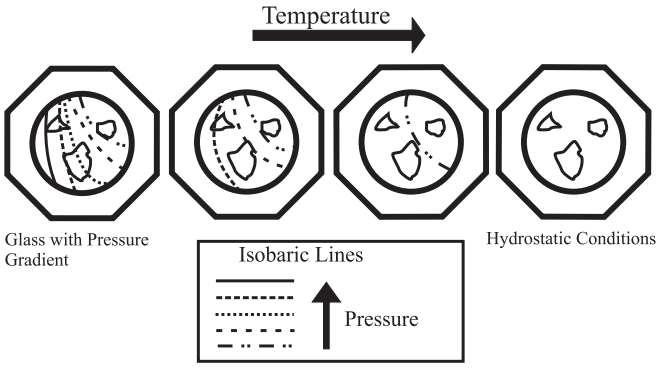

FIG. 1. Schematic glass→liquid transition sequence showing possible initial pressure gradient lines in the DAC sample at low T evolving upon heating until hydrostatic conditions are reached above T_g. Octagonal boundary represents diamond culets (tips of the diamonds), and the smaller circular region represents the sample contained within the steel gasket hole. Three shapes represent rubies at different locations.

cell (DAC). These measurements were performed on the glass-forming liquid cumene up to $P = 4.55$ GPa. We find that Eq. (2) describes the data extremely well yielding a value of γ that holds over the entire pressure range corresponding to a compression of 29%. Furthermore, we take all known temperature and pressure-dependent viscosity data for cumene, corresponding to a dynamic range of 13 orders of magnitude, and show that these data collapse onto a single curve when plotted vs. ρ^γ/T for the same value of γ.

The technique for measuring $T_g(P)$ is based upon the combination of two well-known properties associated with the glass transition. Firstly, a liquid exhibits hydrostatic conditions, whereas compression of a glass leads to a non-uniform stress distribution, manifested by pressure gradients across the sample [28–30]. In a DAC, pressure is measured via fluorescence spectra [31] from small ruby chips placed in different locations in the sample chamber, thereby measuring the pressure various regions. By establishing pressure gradients across a sample in the glass state, and then slowly heating the sample, T_g is determined as the temperature at which the pressure gradients vanish. A schematic of this process is shown in Fig. 1. Isobaric lines show a possible initial state and evolution of stress with increasing temperature. Initial pressure gradients established at low temperature continually decrease upon heating until hydrostatic conditions are reached above T_g.

To further improve accuracy, an additional technique was used based upon the significant increase in the thermal expansivity α_P at T_g when heating into the liquid state. Other PVT experiments have made use of this property to measure T_g through a slope change in isobaric V vs. T curves, but mostly at quite modest pressures [26, 32, 33], with a few notable exceptions up to 1–2 GPa [16, 34]. A DAC is composed of two opposing diamond anvils, which form the top and bottom of the sample chamber, and a cylindrical hole drilled into a metal gasket forms the side walls as shown in Fig. 1. Pressure is easily measured in a DAC, whereas volume is not. When making large temperature changes, precise control of volume or pressure is not possible because of the thermal expansion of the sample, gasket, diamond anvils, and steel anvil holders. However, a slope change is still manifest at T_g in the P vs. T plot, which provides another good marker of the glass transition. This slope change occurs since α_P increases above T_g and the viscous liquid sample expands against the diamonds and gasket walls to a much greater degree than when in the glassy state. With the combination of the two techniques, determination of T_g at high pressure in a DAC is quite accurate.

Cumene (Isopropylbenzene) [$C_6H_5CH(CH_3)_2$ T_m = 177 K, T_g(1 atm) = 127 ± 2 K MW = 120.10 g/mol, purity > 99%] was obtained from Sigma-Aldrich and used as is. It is a good glass former and exhibits an intermediate isobaric fragility $m_P = 70$ at 1 atm [35–37]. It was loaded into a Merrell-Bassett style DAC with a culet size of 500 μm. Stainless steel was used as the gasket material. Ruby fluorescence was used for pressure measurements, and an Argon-Ion 514.5 nm laser line was used as an excitation source. Fluorescence spectra were obtained with a 0.5 m Jarrel-Ash spectrometer and fit according to the method described in Ref. [38], enabling sub-Å resolution and pressure uncertainty of about ± 0.03 GPa. Custom furnace and cryogenic systems were used in the high and low temperature regimes. For each measurement, temperature was initially lowered and then pressure was increased until large differences of at least 0.1 GPa were present between the locations of the three rubies. Temperature was then increased in a stepwise fashion, initially with jumps of 10–15 °C every 30 minutes when the sample was far from the glass transition, and then in steps of 1–2 °C every 15 minutes close to T_g. By incrementing T in this manner, pressure gradients eventually vanish (within uncertainty), after which heating steps were continued for at least another 20 °C. The system was then cooled well below T_g, pressure was increased, and the sample was allowed to equilibrate before beginning the next run.

Four typical heating runs spanning the pressure range of the experiment are shown in Fig. 2. Each starts with pressure differences of $0.2 - 0.6$ GPa at low temperatures in the glassy state. With increasing temperature, the region of highest pressure consistently decreases, while the ruby or rubies at lower pressure show weaker pressure variation as visible in ruby 3 of Figs. 2 (a) and (b). The pressure gradient across the sample decreases until it eventually vanishes (within uncertainty), and hydrostatic conditions are achieved. Coincident with the loss of gradients is a marked increase in the slope dP/dT, most dramatic in the ruby initially at the highest pres-

sure. In low temperature runs (a) and (b), this slope actually changes from negative to positive, showing an increasing pressure for $T > T_g$. Combining the two markers of pressure gradient disappearance and an increase in dP/dT, we obtain measurements of the thermodynamic conditions at the glass transition (T_g, P_g), with estimated uncertainties $(T_g \pm 4\ \mathrm{K}, P_g \pm 0.05\ \mathrm{GPa})$. Values of T_g so determined are shown as vertical dashed lines in Fig. 2.

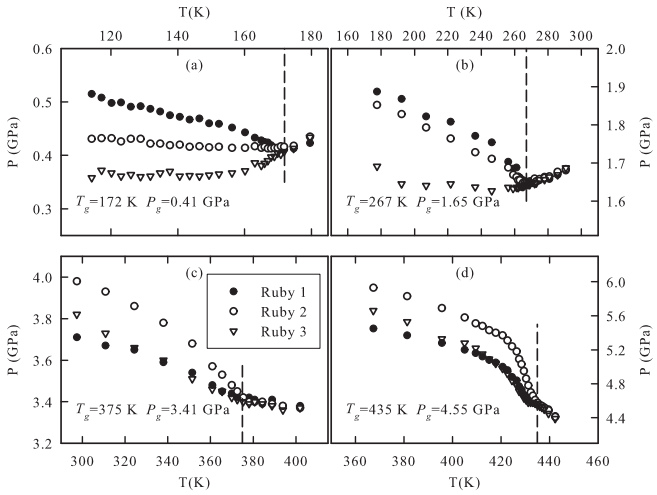

FIG. 2. Four representative glass → liquid transition heating runs. Pressure measurements were obtained from the three rubies arbitrarily designated 1, 2, and 3, as indicated in the legend in the lower right. Runs (a) and (b) were taken with one DAC loading, while (c) and (d) were obtained with a second DAC loading.

The resulting values of T_g thus obtained are shown in Fig. 3 from 26 such heating runs. In the limit of low pressure, the data show excellent agreement with $T_g(1\ \mathrm{bar}) = 127 \pm 2$ K (▲) determined from the average value of several differential thermal analysis experiments [39–41]. Comparison with dynamic measurements show good agreement near room temperature with an estimation of $P_g(293\ \mathrm{K}) \approx 2$ GPa (▼) by Niss [42] who used the high-pressure viscosity data of Li *et al.* [11]. Finally, there is excellent agreement with $P_g(348\ \mathrm{K}) = 2.97$ GPa (◆), determined as the pressure at which $\tau_\alpha(P_g) = 100$ s from high-pressure depolarized light-scattering measurements of τ_α along an isotherm at 75 °C [43]. Strong agreement with both calorimetric and dynamic measurements is good evidence that the current technique is able to measure T_g quite accurately over the very large pressure range of this study.

We fit the $T_g(P)$ data, including the estimation of $T_g(1\ \mathrm{bar}) = 127$ K, to the much used Andersson-Andersson equation [44],

$$T_g(P) = T_{g0}\left(1 + \frac{b}{c}P\right)^{\frac{1}{b}}, \qquad (3)$$

where T_{g0} is the glass transition temperature at atmospheric pressure, and b and c are fitting parameters. A fit of Eq. (3), shown as the solid line in Fig. 3, describes the data quite well over the entire range, with $T_{g0} = 129 \pm 2$ K, $b = 1.67 \pm 0.04$, and $c = 1.16 \pm 0.05$ GPa. The $T_g(P)$ curve corresponds, to a good approximation, to an isochronous line, and should provide dynamic studies of cumene at high pressure with a solid estimation of $\tau_\alpha = 100 - 1000$ s or $\eta = 10^{13} - 10^{14}$ poise at T_g (or P_g) [45]. This will reduce the need for such studies to extrapolate, typically by many orders of magnitude, to T_g, which gives large uncertainty to calculated quantities such as fragility [46], and obfuscates any correlated trends or other conclusions drawn.

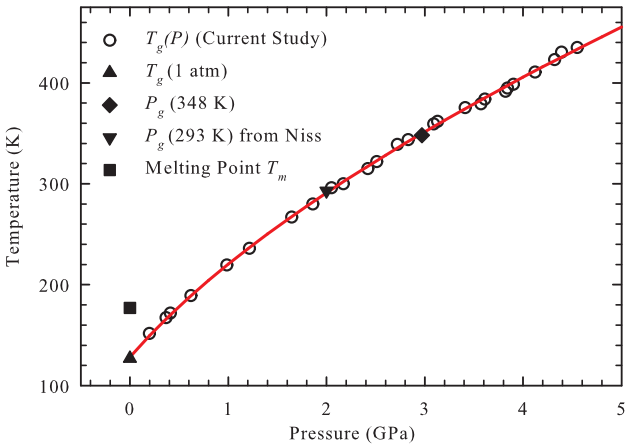

FIG. 3. (Color online) T_g data obtained from 26 heating runs (○). Atmospheric pressure value $T_g(1\ \mathrm{atm}) = 127 \pm 2$ K (▲) is an average of measurements from several sources [39–41]. Atmospheric pressure melting temperature (■) is from Ref. [40]. Value of $P_g(348\ \mathrm{K})$ (◆) was obtained from Ref. [43]. Value of $P_g(293\ \mathrm{K})$ (▼) was obtained from Ref. [42]. Solid line shows fit to Eq. (3).

Our accurate measurements of $T_g(P)$ enable the isochronous testing of density scaling up to extremely high pressures using Eq. (2). The scaling exponent γ is found from the slope of a plot of $\log_{10} T_g$ vs. $\log_{10}\ \rho_g$ shown in the inset of Fig. 4. In order to construct such a plot, a Tait equation of state (EOS) was used based upon measurements by Bridgman up to 4 GPa (see appendix). An excellent linear relationship is indeed evident up to 4.55 GPa, giving no indication that Eq. (2) breaks down at high densities, at least over the range explored here. A linear fit yielded a slope of $\gamma = 4.77 \pm 0.02$. This value is comparable to those found for other non-associated glass-forming liquids [26]. While Eq. (2) predicts $T_g \propto \rho^\gamma$, Dreyfus *et al.* pointed out in Ref. [15] that over limited density ranges it was difficult to differentiate this power-law prediction from other alternatives such as a linear form $T_g \propto \rho - \rho^*$ or a model based upon free volume theory $T_g \propto \rho/(\rho_0 - \rho)$, where ρ_0 is a fitting parameter representing a particular high-density value. It is thus

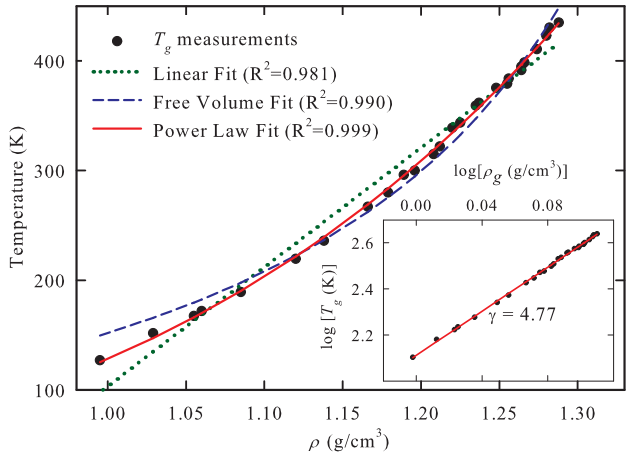

FIG. 4. (Color online) Plot of T_g vs. ρ_g with fits to three models discussed in the text. (Inset) Plot of $\log_{10} T_g$ vs. $\log_{10} \rho_g$ with linear fit.

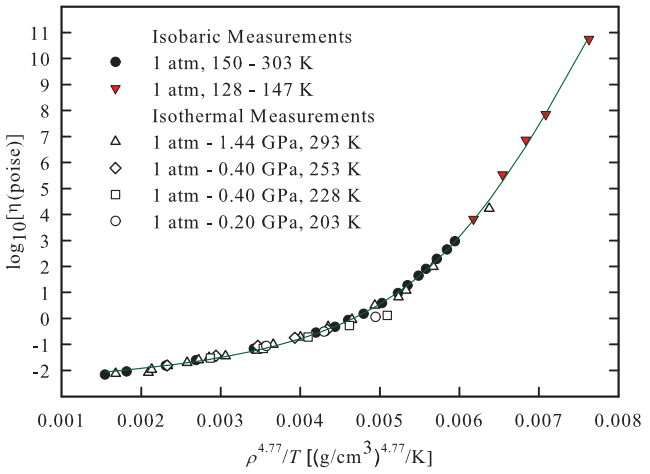

FIG. 5. (Color online) Plot of $\log_{10} \eta$ vs. $\rho^{4.77}/T$ with atmospheric pressure viscosity data from Ref. 35 (●) and Ref. 36 (▼). High pressure isothermal data were obtained from Ref. 11 for 293 K (△), and from Ref. 47 for 253 K (◇), 228 K (□), and 203 K (○). Solid line is fit to Eq. (10) from Ref. [17].

illustrative to plot T_g vs. ρ_g and compare fits to these three functions, shown in Fig. 4. Clearly all three functions can follow general trends of the data (particularly over small compression ranges); however, only the power law prediction is able to describe these data accurately over the full density range covered in this study.

The exponent γ found from the linear fit to $\log_{10} T_g$ vs. $\log_{10}\ \rho_g$ is typically determined by collecting η or τ_α data taken under various thermodynamic conditions, and then iteratively guessing at values of γ until the data superimposes when plotted vs. ρ^γ/T. To test our value of γ from $T_g(P)$ data, we collected previous η measurements from various sources under isothermal and isobaric conditions. Isobaric η measurements were obtained at 1 atm in Ref. 35 down to 150 K and in Ref. 36 down to 130 K, covering a huge dynamic range of 13 orders of magnitude. High pressure isothermal measurements of η up to 0.4 GPa were obtained at 203 K, 228 K, and 253 K in Ref. 47, and up to 1.4 GPa at 293 K in Ref. 11. These data sets are all plotted vs. $\rho^{4.77}/T$ in Fig. 5, where all are found to superimpose in agreement with Eq. (1), noting that the same scaling exponent γ = 4.77 from the isochronous $T_g(P)$ analysis was used. Similar results were also reported in Ref. 42 with γ = 4.85 found from the iterative superposition method.

In summary, direct measurements of $T_g(P)$ using a powerful new method are presented for the glass-forming liquid cumene to pressures up to 4.55 GPa. These data are used for an isochronous density scaling analysis yielding the scaling exponent $\gamma = 4.77 \pm 0.02$. Comparison of several alternative scaling models revealed that only the power law form accurately describes data over this very large compression range of 29%. A density scaling check was then performed with all published viscosity data in cumene at various temperatures and pressures yielding excellent superposition of all data with the same value of γ. Hence, the non-associated liquid cumene is well described by a single scaling parameter over its full dynamic range and over a thermodynamic range heretofore unexplored.

We gratefully acknowledge fruitful discussions with Pradeep Kumar, Mike Roland, and Riccardo Casalini. Financial support was provided from the NSF Division of Materials Research, the Ray Hughes Fellowship, and the University of Arkansas Honors College.

APPENDIX

Bridgman measured the compression of cumene up to 4 GPa at room temperature [48]. Cibulka *et al.* [49] later combined these measurements with other data and fit them with a Tait EOS to model the pressure-dependent density,

$$\rho(T,P) = \frac{\rho_0(T)}{1 - C(T)\,\ln\left(\frac{B(T)+P}{B(T)+0.0001\,\mathrm{GPa}}\right)}, \qquad \text{(A.1)}$$

where $C(T)$ and $B(T)$ are temperature-dependent parameters which drive the EOS, and $\rho_0(T)$ is the atmospheric pressure density. The range of temperature for this EOS given in Ref. [49] is quite restricted, from only 298 K to 333 K, so to better approximate the parameters $C(T)$ and $B(T)$, we borrowed their temperature dependence from toluene (also given in Ref. [49]), which is structurally quite similar to cumene, and has data over a much larger temperature range, from 179 K to 583 K. From the toluene EOS, the parameter $B(T)$ was

increased by 0.007 GPa to overlap with that of cumene in its range, yielding

$$B(T) = \sum_{i=0}^{4} b_i \big[(T - T_0)/100\big]^i$$
$$T_0 = 298.15 \text{ K} \quad \text{and} \quad \vec{b} = \begin{bmatrix} 0.111102 \text{ GPa} \\ -0.080954 \text{ GPa}\cdot\text{K}^{-1} \\ 0.0226 \text{ GPa}\cdot\text{K}^{-2} \\ -0.0034 \text{ GPa}\cdot\text{K}^{-3} \\ 0.00028 \text{ GPa}\cdot\text{K}^{-4} \end{bmatrix} \quad \text{(A.2)}$$

Also, $C(T)$ has a linear dependence for toluene, with a nearly identical value to that of cumene in the 298 K to 333 K range, so it was borrowed with a 20% reduction of the slope dC/dT so that the high temperature behavior of α_P had a more physical pressure dependence, $C(T) = 0.093736 - 0.8\big[(0.005004\,K^{-1})(T - T_0)/100\big]$.

[1] C. A. Angell, Science **267**, 1924 (1995).
[2] G. Adam and J. H. Gibbs, J. Chem. Phys. **43**, 139 (1965).
[3] D. Turnbull and M. H. Cohen, J. Chem. Phys. **52**, 3038 (1970).
[4] M. H. Cohen and G. S. Grest, Annals of the New York Academy of Sciences **371**, 199 (1981).
[5] P. G. Debenedetti and F. H. Stillinger, Nature **410**, 259 (2001).
[6] W. Götze, *Complex Dynamics of Glass-Forming Liquids: A Mode-Coupling Theory*, Vol. 143 (OUP Oxford, 2008).
[7] L. Berthier and G. Biroli, Rev. Mod. Phys. **83**, 587 (2011).
[8] L. Berthier and M. D. Ediger, Physics today **69**, 40 (2016).
[9] H. Weintraub, M. Ashburner, P. N. Goodfellow, H. F. Lodish, C. Arntzen, P. Anderson, T. Rice, T. H. Geballe, A. R. Means, H. M. Ranney, *et al.*, Science **267**, 1615 (1995).
[10] C. M. Roland, S. Hensel-Bielowka, M. Paluch, and R. Casalini, Rep. Prog. Phys. **68**, 1405 (2005).
[11] G. Li, H. E. King Jr, W. F. Oliver, C. A. Herbst, and H. Z. Cummins, Phys. Rev. Lett. **74**, 2280 (1995).
[12] A. Tölle, H. Schober, J. Wuttke, O. G. Randl, and F. Fujara, Phys. Rev. Lett. **80**, 2374 (1998).
[13] R. Casalini and C. M. Roland, Phys. Rev. E **69**, 062501 (2004).
[14] G. Tarjus, D. Kivelson, S. Mossa, and C. Alba-Simionesco, J. Chem. Phys. **120**, 6135 (2004).
[15] C. Dreyfus, A. Le Grand, J. Gapinski, W. Steffen, and A. Patkowski, Eur. Phys. J. B **42**, 309 (2004).
[16] S. Pawlus, R. Casalini, C. M. Roland, M. Paluch, S. J. Rzoska, and J. Ziolo, Phys. Rev. E **70**, 061501 (2004).
[17] R. Casalini and C. M. Roland, Phys. Rev. B **71**, 014210 (2005).
[18] R. Casalini, S. S. Bair, and C. M. Roland, J. Chem. Phys. **145**, 064502 (2016).
[19] C. Alba-Simionesco, A. Cailliaux, A. Alegria, and G. Tarjus, Europhys. Lett. **68**, 58 (2004).
[20] R. Casalini, U. Mohanty, and C. M. Roland, J. Chem. Phys. **125** (2006).
[21] C. Alba-Simionesco and G. Tarjus, J. Non-cryst. Solids **352**, 4888 (2006).
[22] T. B. Schrøder, N. Gnan, U. R. Pedersen, N. P. Bailey, and J. C. Dyre, J. Chem. Phys. **134**, 164505 (2011).
[23] U. R. Pedersen, N. Gnan, N. P. Bailey, T. B. Schrøder, and J. C. Dyre, J. Non-Cryst. Solids **357**, 320 (2011).
[24] T. S. Ingebrigtsen, T. B. Schrøder, and J. C. Dyre, Phys. Rev. X **2**, 011011 (2012).
[25] A. Grzybowski, M. Paluch, K. Grzybowska, and S. Haracz, J. Chem. Phys. **133**, 161101 (2010).
[26] K. Koperwas, A. Grzybowski, K. Grzybowska, Z. Wojnarowska, J. Pionteck, A. P. Sokolov, and M. Paluch, Phys. Rev. E **86**, 041502 (2012).
[27] L. Bøhling, T. S. Ingebrigtsen, A. Grzybowski, M. Paluch, J. C. Dyre, and T. B. Schrøder, New J. Phys. **14**, 113035 (2012).
[28] G. J. Piermarini, S. Block, and J. D. Barnett, J. Appl. Phys. **44**, 5377 (1973).
[29] R. G. Munro, S. Block, and G. J. Piermarini, J. Appl. Phys. **50**, 6779 (1979).
[30] S. Klotz, J. Chervin, P. Munsch, and G. Le Marchand, J. Phys. D: Appl. Phys. **42**, 075413 (2009).
[31] G. J. Piermarini, S. Block, J. D. Barnett, and R. A. Forman, J. Appl. Phys. **46**, 2774 (1975).
[32] M. Paluch, J. Chem. Phys. **115**, 10029 (2001).
[33] Z. Wojnarowska, M. Paluch, A. Grzybowski, K. Adrjanowicz, K. Grzybowska, K. Kaminski, P. Wlodarczyk, and J. Pionteck, J. Chem. Phys. **131**, 104505 (2009).
[34] M. S. Elsaesser, I. Kohl, E. Mayer, and T. Loerting, J. Phys. Chem. B **111**, 8038 (2007).
[35] A. J. Barlow, J. Lamb, and A. J. Matheson, in *Proc. R. Soc. A*, Vol. 292 (The Royal Society, 1966) pp. 322–342.
[36] A. C. Ling and J. E. Willard, J. Phys. Chem. **72**, 1918 (1968).
[37] L. Wang, C. A. Angell, and R. Richert, J. Chem. Phys. **125**, 74505 (2006).
[38] R. G. Munro, G. J. Piermarini, S. Block, and W. B. Holzapfel, J. Appl. Phys. **57**, 165 (1985).
[39] M. R. Carpenter, D. B. Davies, and A. J. Matheson, J. Chem. Phys. **46**, 2451 (1967).
[40] G. P. Johari and M. Goldstein, J. Chem. Phys. **53**, 2372 (1970).
[41] S. S. N. Murthy, S. K. Nayak, *et al.*, J. Chem. Soc., Faraday Trans. **89**, 509 (1993).
[42] K. Niss, *Fast and slow dynamics of glass-forming liquids*, Ph.D. thesis, Universite Paris-Sud (2007).
[43] T. C. Ransom, W. F. Oliver, and K. Lyon, (unpublished).
[44] S. P. Andersson and O. Andersson, Macromolecules **31**, 2999 (1998).
[45] Because the time scales for these experiments are on the order of a few minutes, T_g values thus determined may be better described by a larger τ_α or η value.
[46] S. Pawlus, M. Paluch, J. Ziolo, and C. M. Roland, J. Phys.: Condens. Matter **21**, 332101 (2009).
[47] I. Artaki and J. Jonas, J. Chem. Phys. **82**, 3360 (1985).
[48] P. W. Bridgman, in *P. Am. Acad. Arts Sci.* (JSTOR, 1949) pp. 129–146.
[49] I. Cibulka and T. Takagi, J. Chem. Eng. Data **44**, 411 (1999).